Heliyon 10 (2024) e33314

Contents lists available at ScienceDirect

Heliyon

journal homepage: www.cell.com/heliyon

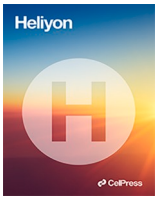

Research article

Sinomenine ameliorates bleomycin-induced pulmonary fibrosis by inhibiting the differentiation of fibroblast into myofibroblast

Zuqiong Nie [1], Jing Wu [1], Jun Xie, Wanling Yin [*]

Department of Geriatrics, The Central Hospital of Wuhan, Tongji Medical College, Huazhong University of Science and Technology, Wuhan, 430014, China

ARTICLE INFO

Keywords:
Pulmonary fibrosis
Sinomenine
Fibroblasts
Myofibroblasts
Aerobic glycolysis

ABSTRACT

Idiopathic pulmonary fibrosis (IPF) represents a severe interstitial lung disease characterized by limited therapeutic interventions. Recent study has suggested that sinomenine (SIN), an alkaloid derived from the roots of Sinomenium acutum, demonstrates efficacy in interrupting aerobic glycolysis, a predominant metabolic pathway in myofibroblasts. However, its pharmacological potential in the context of pulmonary fibrosis remains inadequately explored. In the present study, we established a bleomycin (BLM)-induced pulmonary fibrosis mouse model and subjected the mice to a one-week regimen of SIN treatment to assess its efficacy. Additionally, a TGF-β1-induced primary lung fibroblast model was employed to investigate the molecular mechanism underlying the effects of SIN. Our observations revealed robust anti-pulmonary fibrosis properties associated with SIN treatment, as evidenced by reduced extracellular matrix deposition, diminished hydroxyproline contents, improved Ashcroft scores, and enhanced lung function parameters. Furthermore, SIN administration significantly impeded TGF-β1-induced fibroblast-to-myofibroblast differentiation. Mechanistically, SIN exerted its beneficial effects by mitigating aerobic glycolysis, achieved through the inhibition of the expression of 6-phosphofructo-2-kinase/fructose-2,6-bisphosphatase 3 (Pfkfb3). Notably, the protective effects of SIN on fibroblasts were reversed upon ectopic overexpression of Pfkfb3. In conclusion, our data underscore the potential of SIN to attenuate fibroblast-to-myofibroblast differentiation by modulating Pfkfb3-associated aerobic glycolysis and SIN emerges as a promising anti-fibrotic agent for pulmonary fibrosis in clinical practice.

1. Introduction

Idiopathic pulmonary fibrosis (IPF) is a chronic, progressive, and fibrotic interstitial lung disease with an uncertain etiology [1]. The condition is distinguished by persistent alveolar type II epithelial injury, myofibroblast formation and excessive deposition of extracellular matrix (ECM) in the lung parenchyma [1,2]. Despite the FDA approval of nintedanib and pirfenidone for IPF treatment, these pharmaceuticals only attenuate the decline in lung function and do not reverse or halt the fibrotic process [3]. Consequently, the median survival rate post-IPF diagnosis ranges from 3 to 5 years, emphasizing the critical need for innovative therapeutic options.

* Corresponding author. Department of Geriatrics, The Central Hospital of Wuhan, Tongji Medical College, Huazhong University of Science and Technology, China.
E-mail address: yinwanling@zxhospital.com (W. Yin).
[1] These authors contributed equally to this work.

https://doi.org/10.1016/j.heliyon.2024.e33314
Received 18 March 2024; Received in revised form 17 June 2024; Accepted 19 June 2024
Available online 24 June 2024

While the precise pathogenesis of IPF remains elusive, substantial evidence implicates myofibroblasts as pivotal effectors in disease progression [4,5]. Within fibrotic microenvironments, myofibroblasts, predominantly derived from fibroblasts, generate an abundance of ECM, including fibronectin and collagen proteins, leading to impaired gas exchange, respiratory failure, and eventual mortality [6]. Targeting myofibroblast formation is thus a crucial avenue for pharmaceutical development in IPF.

Sinomenine (SIN), extracted from the traditional Chinese medicine Sinomenium acutum, has gained recognition for its diverse pharmacological actions, encompassing anti-inflammatory, immunosuppressive, antitumor, neuroprotective, and antiarrhythmic effects [7]. A recent study elucidated SIN's profound inhibitory effect on human non-small cell lung cancer cells by attenuating aerobic glycolysis, colloquially known as the "Warburg effect" [8]. Aerobic glycolysis, characterized by increased glucose uptake and lactate production in the presence of oxygen, emerges as the predominant metabolic pathway in lung myofibroblasts during pulmonary fibrosis progression [9,10]. Inhibition of aerobic glycolysis has been associated with diminished fibroblast-to-myofibroblast differentiation and improved pulmonary fibrosis [9,10]. However, the involvement of SIN in the dysregulated aerobic glycolysis of myofibroblasts during the progression of pulmonary fibrosis remains unknown.

In this study, we elucidate that administration of SIN significantly protects mice from bleomycin (BLM)-induced pulmonary fibrosis by mitigating fibroblast-to-myofibroblast differentiation. Mechanistically, SIN exerts its beneficial effects by suppressing aerobic glycolysis through the inhibition of 6-phosphofructo-2-kinase/fructose-2,6-bisphosphatase 3 (Pfkfb3), which catalyzes the conversion of fructose-6-phosphate to fructose-2,6-bisphosphate—an allosteric activator of PFK1 and a potent glycolysis stimulator [11]. Importantly, the protective effects of SIN on fibroblasts are reversed upon Pfkfb3 overexpression. Collectively, this study establishes SIN as a promising anti-fibrotic agent for pulmonary fibrosis in clinical practice.

2. Materials and methods

2.1. Materials

SIN and BLM were procured from MedChemExpress (NJ, USA). Recombinant mouse TGF-β1 was obtained from PeproTech (NJ, USA). Antibodies targeting fibronectin, Collagen I, α-SMA, and β-actin were sourced from Cell Signaling Technology, Inc. (MA, USA). Antibodies against Pfkfb3, Hk2, and Ldha were acquired from Santa Cruz Biotechnology (CA, USA). The RT-PCR assay kit was supplied by Dalian Takara Company (Dalian, China), and Cell Counting Kit-8 (CCK8) was purchased from Dojindo Chemical Technology Co. Ltd. (Shanghai, China). L-lactate assay kit and hydroxyproline assay kit were provided by Sigma-Aldrich (MO, USA).

2.2. Bleomycin model of pulmonary fibrosis and SIN administration

Eighty-five male C57BL/6 mice (eight weeks old) were obtained from Beijing Charles River Laboratory Animal Technology Co., Ltd. (Beijing, China) and housed in a specific pathogen-free (SPF) environment. Ethical approval for all animal experiments was granted by the Ethics Committee of Tongji Medical College, Huazhong University of Science and Technology. Mice were randomly allocated to four groups: 1. PBS group; 2. BLM group; 3. PBS + SIN group; 4. BLM + SIN group. Initial anesthesia was induced with intraperitoneal injection of pentobarbital sodium (60 mg/kg), followed by intratracheal injection of BLM (1.5 mg/kg) in PBS or an equivalent volume of PBS [12]. SIN (100 mg/kg) was administered orally daily for 7 days starting from the second week post-BLM injection (Fig. 1). Mice were euthanized on day 21 following BLM challenge.

2.3. Histopathology

The left mouse lungs underwent perfusion with 4 % neutral buffered paraformaldehyde, followed by storage at room temperature for 24 h and subsequent paraffin embedding. Lung sections of 5 μm thickness were prepared and stained with hematoxylin-eosin (H&E) and Sirius red. Histopathological examination was performed using light microscopy, and the Ashcroft score was utilized for a blinded assessment of pulmonary fibrosis severity, following established protocols [13].

2.4. Hydroxyproline assay

The determination of hydroxyproline concentration in the lungs followed the manufacturer's instructions. In summary, lung tissues were subjected to hydrolysis with 12 M hydrochloric acid at 120 °C for 3 h, followed by incubation with DMAB reagent at 60 °C for 90 min. Subsequently, hydroxyproline levels were assessed using colorimetric spectrophotometry (ELx800, BioTek Instruments, Inc., Winooski, VT) at a wavelength of 560 nm with a microplate meter, following the addition of the stop solution.

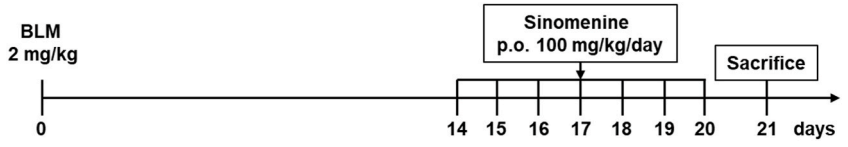

Fig. 1. Time course of BLM and SIN administration.

2.5. Cell culture and treatment

Primary mouse lung fibroblasts were isolated from 1-week-old C57BL/6 mouse lung tissues following established protocols [14]. The tissues underwent digestion with collagenase type I (20 mg/ml) in Hanks' Balanced Salt Solution (HBSS) for 1 h at 37 °C. Following centrifugation, cells were resuspended in DMEM containing 10 % fetal bovine serum (FBS) and penicillin/streptomycin at 37 °C. Fibroblasts were then treated with TGF-β1 (10 ng/ml) or SIN (50 μM) for 24 h. Pfkfb3-plasmid (1.5 μg) or vector plasmid was transfected into fibroblasts using Lipo-3000, and cellular analysis was performed by RT-PCR 48 h post-transfection.

2.6. Western blot

Lung tissues or fibroblasts were homogenized and lysed with RIPA buffer (Beyotime, Shanghai, China) following previously established described [15]. After centrifuged, the supernatants were collected and boiled for 5 min. The primary antibodies used were anti-fibronectin (1:1000); anti-Collagen I (1:1000), *anti*-α-SMA (1:1000), *anti*-β-actin (1:2000); anti-Pfkfb3 (1:1000), *anti*-Hk2 (1:1000) and *anti*-Ldha(1:1000). β-actin served as the loading control, and blots were visualized using an enhanced chemiluminescence system (Bio-Rad, USA). Gray values were analyzed with ImageJ software.

2.7. Real-time PCR

Total RNA was extracted from lung tissues and fibroblasts using TRIzol reagent as previously reported [16]. Subsequently, the RNA quantity and quality were assessed using a NanoDrop 2000 spectrophotometer (Thermo Scientific, MA, USA). The RNA underwent reverse transcription into cDNA using a reverse transcription kit and was then subjected to Real-time PCR analysis with Maxima SYBR Green qPCR Master Mix. Actb RNA levels were utilized for data normalization, and quantification was executed using the comparative CT method (ΔΔCT). The following primers were employed: Forward, 5′-GTG TTT TCC ACG GAT GCT G-3′ and reverse, 5′- TGC CCA CTG CTG ACT TAG G-3′ for *Fn1*; Forward, 5′- GCG AGT GCT GTG CTT TCT G -3′ and reverse, 5′- AGG ACA TCT GGG AAG CAA A-3′ for *Col1a1*; Forward, 5′-GGC TTC GCT GGT GAT GAT GCT C-3′ and reverse, 5′- TCC CTC TCT TGC TCT GGG CTT C-3′ for *Acta2*; Forward, 5′- CAA CTC CCC AAC CGT GAT TGT -3′ and reverse, 5′- GAG GTA GCG AGT CAG CTT CTT -3′ for *Pfkfb3*; Forward, 5′- GTG ACG TTG ACA TCC GTA AAG A -3′ and reverse, 5′- GCC GGA CTC ATC GTA CTC C-3′ for *Actb*.

2.8. Lactate assay

Equal numbers of fibroblasts were plated in 12-well plates overnight, and lactate levels in the collected suspension were determined using a lactate assay kit following the manufacturer's protocol.

2.9. Lung mechanics measurements

The lung mechanics were assessed using a flexiVent system (SCIREQ, Inc., Montreal, QC, Canada) following previously established methods [17]. Briefly, mice were anesthetized with pentobarbital sodium (80 mg/kg, i. p.), and tracheotomy was performed to connect the mice with the flexiVent system. Ventilation was conducted at a breathing rate of 150 breaths/min with a tidal volume of 10 ml/kg, utilizing a positive end-expiratory pressure (PEEP) of 3 cmH2O, facilitated by a computer-controlled small-animal ventilator. The SINapshot-150 was employed to measure the total respiratory system resistance (Rrs), compliance (Crs), and elastance of the respiratory system (Ers). G and H values were acquired through Quick Prime-3. Subsequently, all data underwent analysis using SCIREQ flexiWare (version 7.6, service pack 5, SCIREQ).

2.10. The detection arterial blood gas

Arterial blood samples were subjected to analysis using an automatic blood gas analyzer (ABL80, Radiometer, Copenhagen, Denmark) immediately after collection via left ventricle puncture as previously reported [18].

2.11. Assessment of liver function and renal function

In order to assess the biosafety of SIN in vivo, blood samples were obtained from mice via cardiac puncture and subsequently centrifuged at 3000 g for 5 min to isolate serum. The serum was then analyzed for levels of aspartate aminotransferase (AST), alanine aminotransferase (ALT), urea, and creatinine (Cr) using commercially available test kits from Abcam (Cambridge, UK), following the manufacturer's instructions.

2.12. Bioenergetic assay

A Seahorse Bioscience Extracellular Flux Analyzer (XFe96, Seahorse Bioscience Inc., North Billerica, MA, USA) was employed to monitor the extracellular acidification rate (ECAR) and oxygen consumption rate (OCR) of fibroblasts [11]. Briefly, fibroblasts were initially seeded in an XF24 culture plate and exposed to various stimuli for a 24-h period. Before measurements were taken, the growth media were replaced with DMEM without FBS and sodium bicarbonate. The cells were then incubated in a CO2-free environment at

37 °C for 1 h. For the ECAR assay, the medium received additions of 10 mM glucose, 1 μM oligomycin, and 75 mM 2-deoxy-glucose (2-DG) from the XF Glycolysis Stress Test kit (103020, Agilent, Santa Clara, CA, USA). In the OCR assay, the medium was injected with 1 μM oligomycin, 1 μM carbonyl cyanide-phospho-(p)-trifluoro-methoxyphenyl-hydrazon (FCCP), and 0.5 μM rotenone/antimycin A from the XF Mito Stress Test kit (103015-100, Agilent, Santa Clara, CA, USA). Subsequently, all OCR and ECAR values underwent normalization as per the Seahorse Normalization protocol.

2.13. Statistical analysis

Results were shown as the mean ± standard deviation (SD). Data analysis was performed using GraphPad Prism 8. A two-tailed unpaired *t*-test determined significance between two groups, and one-way Analysis of Variance (ANOVA) for multiple comparisons using Tukey's post hoc test was applied for comparisons among three or more groups.

3. Results

3.1. SIN administration reduces the progression of BLM-induced pulmonary fibrosis

To evaluate the impact of SIN on pulmonary fibrosis, a murine model was established through intratracheal administration of BLM. Firstly, the potential toxicity of SIN was examined through blood biochemistry analyses. Importantly, SIN exhibited no significant toxicity to mice, as indicated by the plasma concentration of alanine aminotransferase (ALT, Fig. 2A), aspartate aminotransferase (AST,

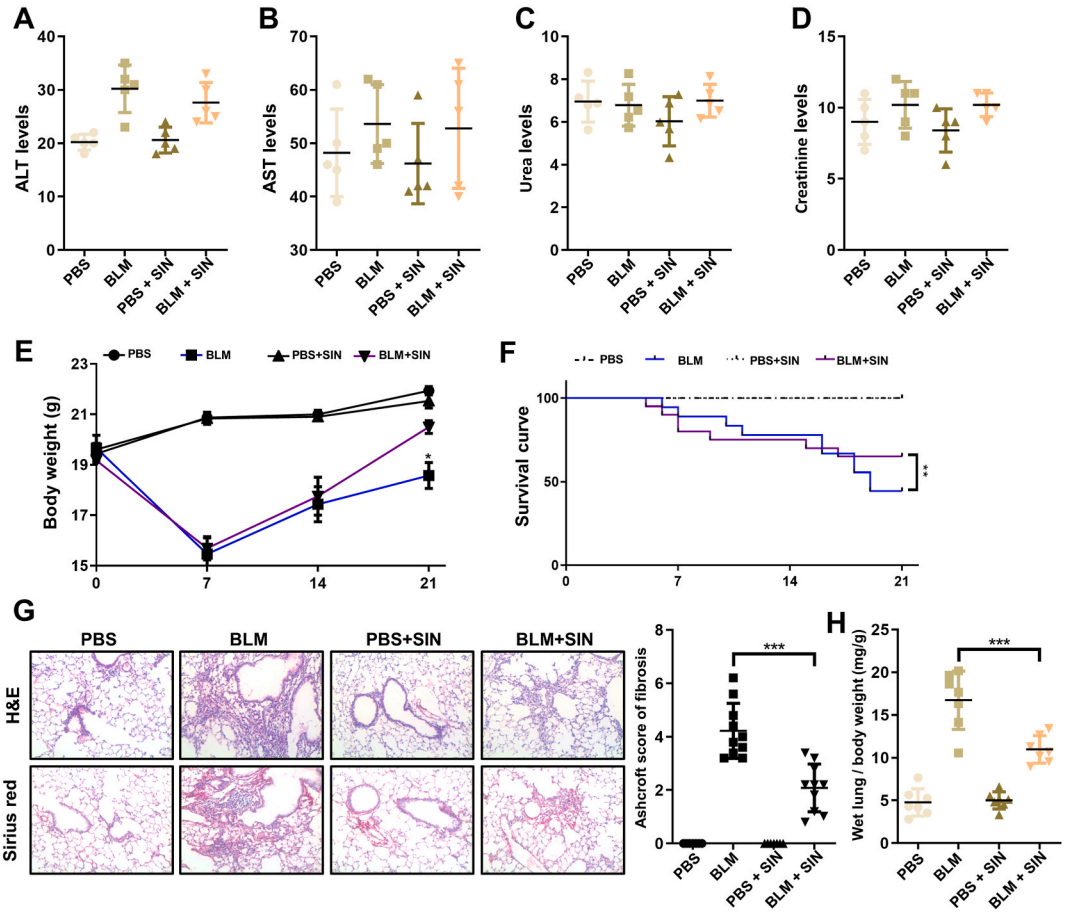

Fig. 2. SIN administration attenuates BLM-induced pulmonary fibrosis. A-B: The plasma concentration of alanine aminotransferase (ALT, A) and aspartate aminotransferase (AST, B) in each group; C-D: The plasma concentration of Urea (C) and Creatinine (D) in each group; E: Body weight change during the course of BLM-induced fibrosis; F: The survival curve of all mice studied; G: Histological analysis for the severity of lung fibrosis in mice after BLM induction. Left panel: representative results for H&E (Up), Sirius red (Down). Right panel: a bar graph showing the semiquantitative Ashcroft scores for the severity of fibrosis. Images were taken under original magnification × 200. H: The ratio of wet lung and body weight. Each bar represents mean ± SD of 5–10 mice analyzed. *$p < 0.05$; **$p < 0.01$; ***$p < 0.001$. (For interpretation of the references to color in this figure legend, the reader is referred to the Web version of this article.)

Fig. 2B), Urea (Fig. 2C) and Creatinine (Fig. 2D). While the body weight in the BLM-treated groups initially decreased and gradually recovered after day 8 (Fig. 2E), oral administration of SIN significantly mitigated the weight loss (Fig. 2E). Notably, SIN also enhanced survival in mice with pulmonary fibrosis (Fig. 2F). Histological examinations, including H&E and Sirius red staining, revealed severe damage to alveolar structures, alveolar wall thickening, and collagen deposition in the BLM group compared to the PBS group. However, oral administration of SIN markedly attenuated these effects, evidenced by a reduced Ashcroft score (Fig. 2G). Additionally, SIN treatment effectively reduced the relative lung weight (Fig. 2H).

Subsequently, Western blot analyses were conducted to assess the expression of fibrotic proteins. The results demonstrated a significant reduction in the expression of fibronectin, collagen I, and α-SMA in the lung tissues of mice with pulmonary fibrosis following oral administration of SIN (Fig. 3A). Similar findings were observed through RT-PCR (Fig. 3B–D). Consistent with these data, SIN administration also led to a decrease in hydroxyproline content in the lung tissue of mice with pulmonary fibrosis (Fig. 3E). Collectively, these results indicate that SIN has the potential to mitigate the progression of BLM-induced pulmonary fibrosis.

3.2. SIN treatment preserves pulmonary function in BLM-induced mice

To comprehensively assess the effects of SIN on pulmonary fibrosis, we conducted a thorough analysis of the mechanical dynamics of the respiratory system. BLM-treated mice exhibited a substantial reduction in distensibility (Cst, Fig. 4A) and compliance (Crs, Fig. 4B) of the total respiratory system, accompanied by an elevation in elastance (Ers, Fig. 4C) and resistance (Rrs, Fig. 4D) of the total respiratory system compared to the PBS control. Similar trends were observed in the damping of tissue (G, Fig. 4E) and the elastance of tissue (H, Fig. 4F). Remarkably, the pulmonary function in the BLM + SIN group showed significant improvement compared to that in the BLM group, indicating that SIN treatment attenuated BLM-induced pulmonary dysfunction (Fig. 4A–F).

To further evaluate pulmonary function, arterial blood gas analysis was performed. Consistently, lower arterial oxygen partial pressure (PaO2) and higher arterial carbon dioxide partial pressure (PaCO2) were observed in the BLM group compared with the PBS group (Fig. 4G and H). However, these alterations were significantly ameliorated following SIN administration in BLM-treated mice (Fig. 4G and H). Taken together, these data demonstrate that SIN administration effectively mitigated bleomycin-induced pulmonary dysfunction.

3.3. SIN attenuates TGF-β1 induced fibroblast to myofibroblast differentiation

To evaluate the impact of SIN on myofibroblast formation, a pivotal cellular process in pulmonary fibrosis, primary mouse lung fibroblasts were cultured. Initially, we investigated the influence of various concentrations of SIN on fibroblast viability. Results demonstrated that even at a high concentration of 400 μM, SIN did not adversely affect fibroblast viability (Fig. 5A). Subsequently, cells were treated with TGF-β1 and SIN (50 μM) for 24 h. The data revealed an elevation in the expression of fibrosis-related genes (Fig. 5B) and proteins (Fig. 5C) upon TGF-β1 stimulation. However, following SIN treatment, the aforementioned indicators exhibited

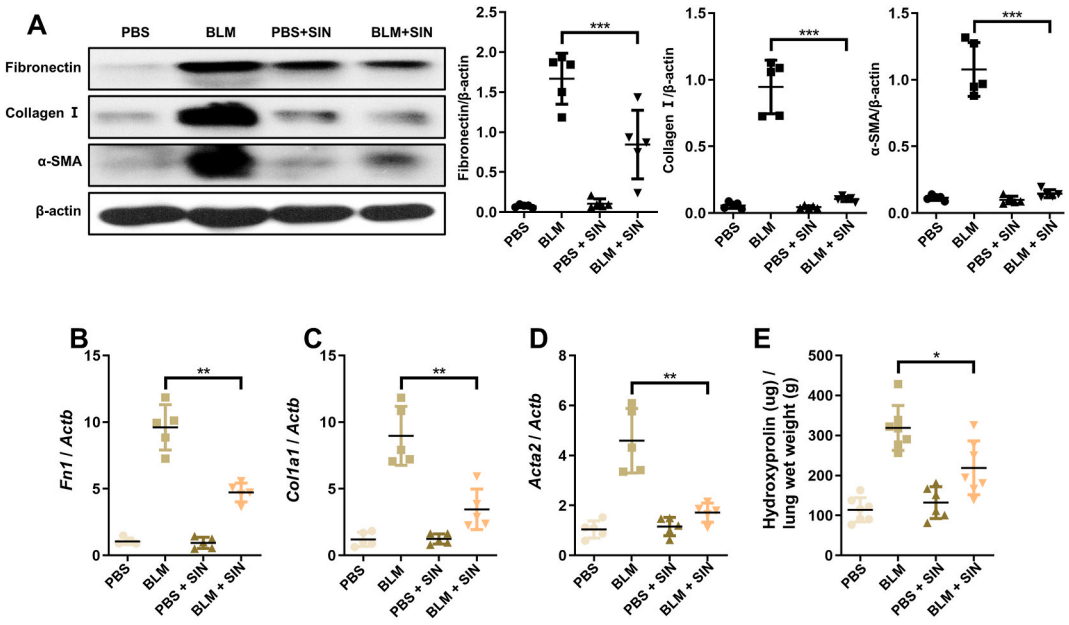

Fig. 3. SIN treatment abrogates fibrotic markers expression following BLM injection. A: Western blot analysis of fibronectin, collagen I and α-SMA expression. Left panel: representative Western blot results. Right panel: bar graphs showing the mean data of all mice analyzed in each group. B-D: RT-PCR analysis of *Fn1* (B), *col1a1* (C) and *Acta2* (D) expression. E: The rates of hydroxyproline and lung wet weight of all mice studied. Each bar represents mean ± SD of 5 mice analyzed. *$p < 0.05$; **$p < 0.01$; ***$p < 0.001$.

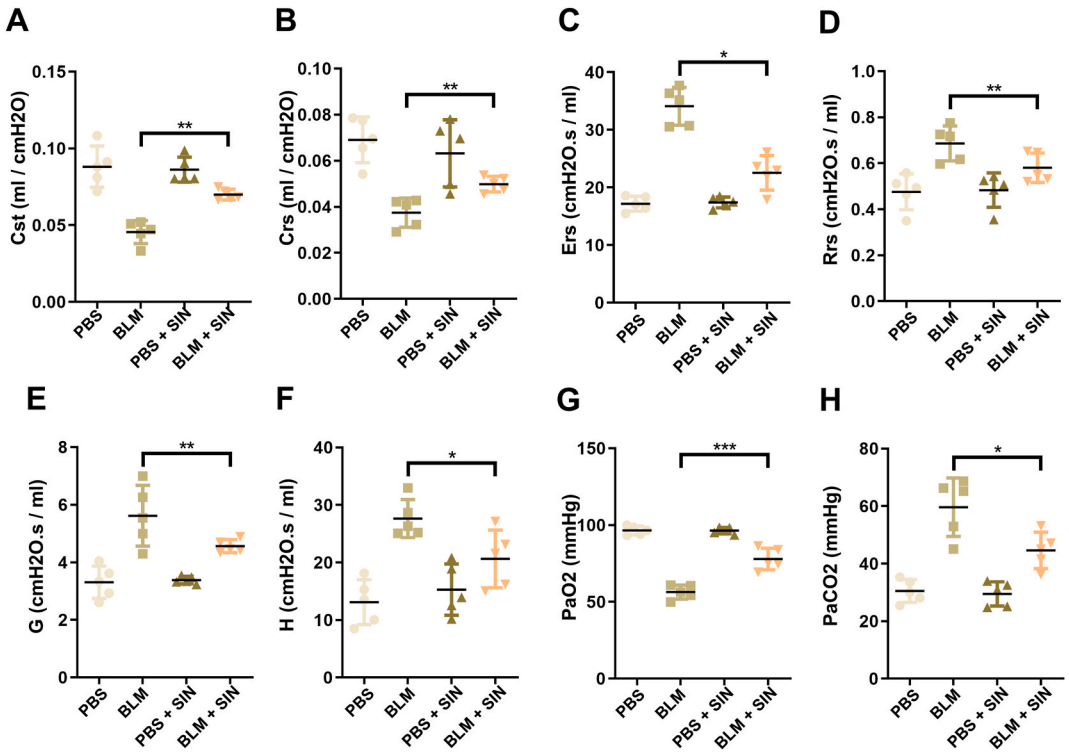

Fig. 4. The protection effects of SIN on pulmonary function in BLM-induced mice. A-F: The lung functional analysis using flexiVent system. Quasi-static compliance (Cst, A), Compliance respiratory system (Crs, B), Elastance of the respiratory system (Ers, C), Resistance of the respiratory system (Rrs, C), Tissue damping (G, E), Tissue elastance (H, F); G-H: Arterial blood gas analysis of PaO2 (G) and PaCO2 (H). Each bar represents mean ± SD of 5 mice analyzed. $^{*}p < 0.05$; $^{**}p < 0.01$; $^{***}p < 0.001$.

a significant decrease compared to the TGF-β1-stimulated group. This suggests that SIN effectively inhibits the transformation of fibroblasts into myofibroblasts.

3.4. SIN blunts aerobic glycolysis in TGF-β1 induced fibroblast via regulating Pfkfb3 expression

To investigate the effects of SIN on TGF-β1-induced metabolic reprogramming, we employed the Seahorse Bioscience Extracellular Flux Analyzer to monitor the extracellular acidification rate (ECAR) and oxygen consumption rate (OCR) of fibroblasts following TGF-β1 and SIN treatment. Consistent with previous studies [11,19], TGF-β1 treatment significantly enhanced glycolysis and glycolytic activity (Fig. 6A–C), while attenuating basal respiration and maximal respiration (Fig. 6F–H), indicative of the fibroblasts undergoing an aerobic glycolytic program (Fig. 6I). Conversely, administration of SIN significantly reversed the aerobic glycolytic program induced by TGF-β1 (Fig. 6A-C and F–I). In line with these findings, SIN significantly decreased lactic acid levels in fibroblasts (Fig. 6D) and fibrotic lung tissues (Fig. 6E).

To elucidate the mechanism by which SIN regulates aerobic glycolysis, we examined the expression of key enzymes of the glycolytic pathway. TGF-β1 upregulated the expression of Pfkfb3, HK2, and Ldha at the protein and mRNA levels (Fig. 7A and B). However, SIN treatment specifically attenuated the expression of Pfkfb3, while HK2 and Ldha remained unaffected (Fig. 7A and B). Furthermore, the expression of Pfkfb3 in the lung tissues of mice with pulmonary fibrosis was significantly mitigated by oral administration of SIN (Fig. 7C and D), suggesting that SIN may attenuate aerobic glycolysis by reducing Pfkfb3 expression. To further confirm these results, we constructed a Pfkfb3 plasmid to overexpress Pfkfb3 (Fig. 7E). Fibroblasts were transfected with Pfkfb3 plasmid or vector plasmid before SIN and TGF-β1 treatment. Importantly, the protective effects of SIN on fibroblast to myofibroblast differentiation were mitigated after Pfkfb3 overexpression. Furthermore, upregulating Pfkfb3 significantly reversed the decrease in extracellular lactic acid levels in SIN-treated fibroblasts. These data suggest that SIN blunts fibroblast activation by repressing TGF-β1-induced Pfkfb3-mediated glycolysis.

4. Discussion

IPF represents a persistent and life-threatening interstitial lung disease characterised by the activation of fibroblasts, excessive deposition of the extracellular matrix, and the formation of scar tissue within the lungs [20]. Although the FDA has sanctioned the use of nintedanib and pirfenidone for IPF treatment, these medications exhibit limited efficacy in reducing patient mortality [21].

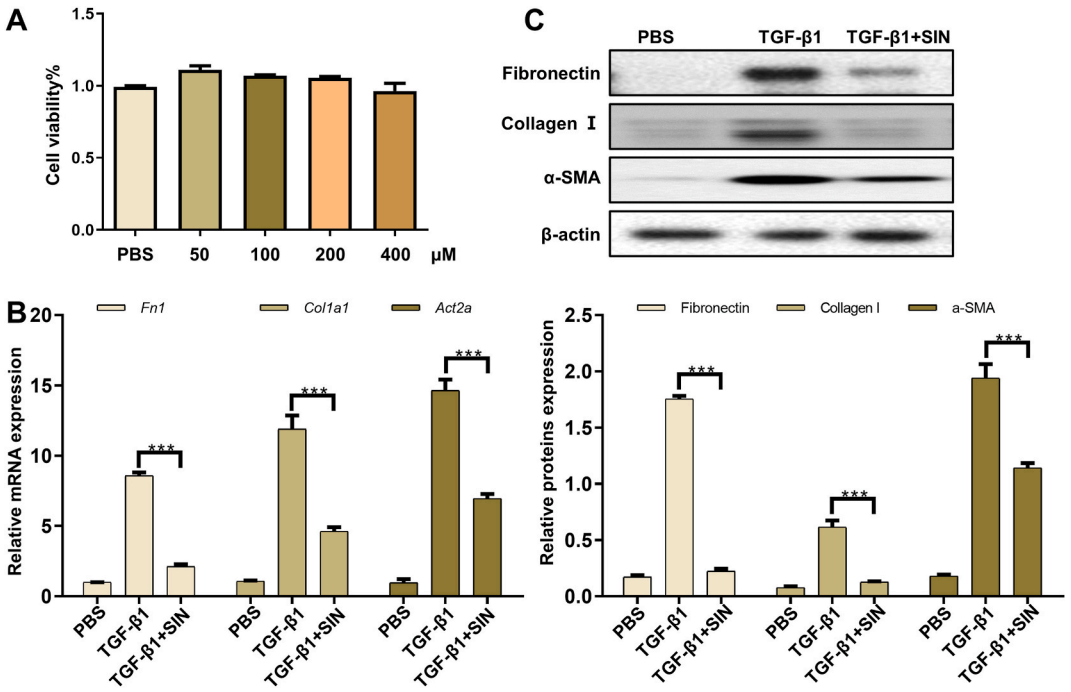

Fig. 5. SIN treatment inhibited fibroblast differentiation. A: Cell viability in primary mouse lung fibroblasts tested by CCK8 stimulated with different doses of SIN for 24 h; B: RT-PCR analysis of Fn1, col1a1 and Acta2 expression. C: Western blot analysis of fibronectin, collagen I and α-SMA expression. Up panel: representative western blotting results. Down panel: figures showing the data with three replications. Each bar represents mean ± SEM of three replications analyzed. $^{***}p < 0.001$.

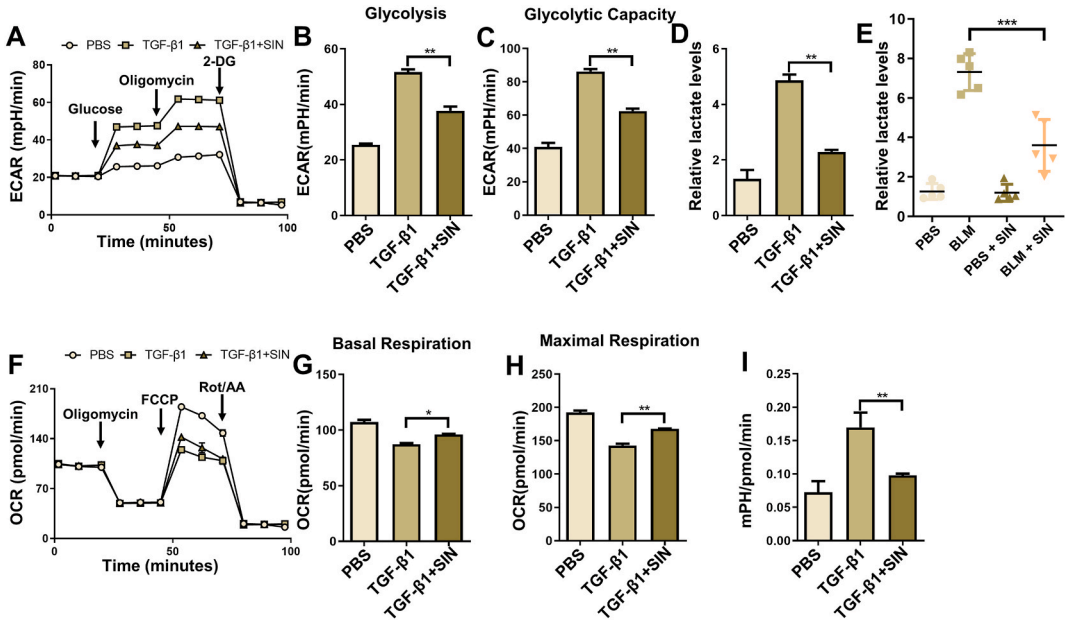

Fig. 6. administration of SIN attenuates aerobic glycolysis in TGF-β1 induced fibroblast. A: ECAR was measured using Seahorse; B–C: Glycolysis (B) and glycolysis capacity (C) are quantified and shown as histograms; D-E: Relative lactate levels in fibroblasts (D) and fibrotic lungs (E); F: OCR was measured using Seahorse; G-H: Basal respiration (G) and maximal respiration (H) are quantified and shown as histograms; I: The ratio of mean ECAR and OCR. Each bar represents mean ± SEM of three replications analyzed. $^{*}p < 0.05$; $^{**}p < 0.01$; $^{***}p < 0.001$.

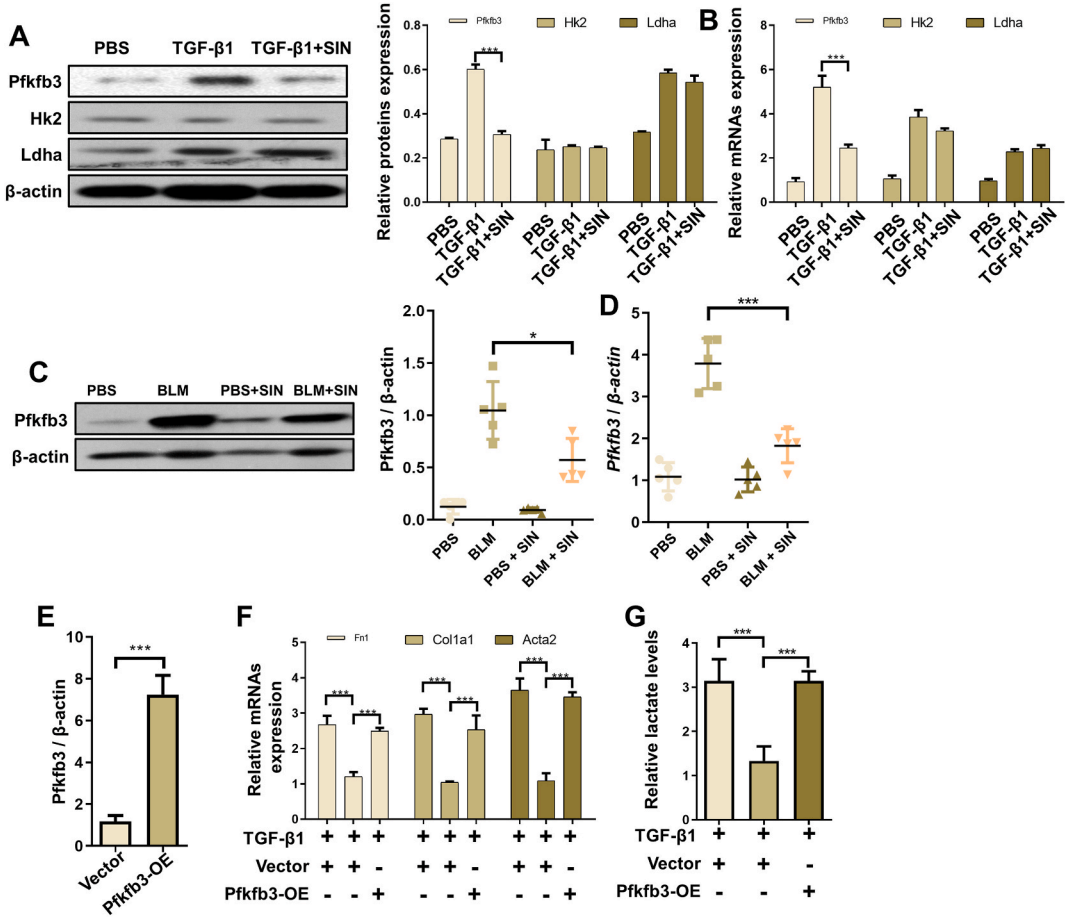

Fig. 7. SIN reduces aerobic glycolysis by regulating Pfkfb3 expression. A: Western blot analysis of Pfkfb3, Hk2 and Ldha expression. Left panel: representative Western blot results. Right panel: figures showing the data with three replications. B: RT-PCR analysis of *Pfkfb3*, *Hk2* and *Ldha* expression. C: Western blot analysis of Pfkfb3 expression in the lung. Left panel: a representative Western blot result. Right panel: A bar graph showing the mean data of all mice analyzed in each group. D: RT-PCR analysis of *Pfkfb3* expression in the lung. E: RT-PCR analysis of *Pfkfb3* expression in fibroblast after *Pfkfb3* plasmid transfected. F: RT-PCR analysis of Fn1, col1a1 and Acta2 expression in TGF-β1 induced fibroblasts after *Pfkfb3* plasmid transfected. H: Relative lactate levels in TGF-β1 induced fibroblasts after *Pfkfb3* plasmid transfected. Each bar represents mean ± SEM of three replications analyzed. *$p < 0.05$; ***$p < 0.001$.

Consequently, there arises a pressing need for innovative therapeutic approaches in the prevention and management of pulmonary fibrosis. In this investigation, we unveiled robust anti-pulmonary fibrosis properties associated with SIN treatment. These properties were substantiated by a reduction in extracellular matrix deposition, diminished hydroxyproline contents, improved Ashcroft scores, and enhanced lung function parameters. Notably, SIN administration significantly impeded TGF-β1-induced fibroblast-to-myofibroblast differentiation. Mechanistically, SIN manifested its beneficial effects by mitigating aerobic glycolysis, achieved through the inhibition of Pfkfb3 expression. Importantly, the protective effects of SIN on fibroblasts were nullified upon ectopic overexpression of Pfkfb3. This study posits SIN as a potential therapeutic agent for pulmonary fibrosis.

SIN, an isoquinoline alkaloid monomer derived from the traditional Chinese medicine Menispermaceae plant Sinomenium acutum, is primarily found in hydrochloride form [7]. Historically, SIN has been employed in Chinese medicine for centuries to treat arthritis due to its regulatory impact on the secretion of multiple inflammatory cytokines and immune cells [22]. Recent research has expanded the understanding of SIN's pharmacological activities, encompassing anti-tumor [23] and neuroprotective functions [24]. Feasible evidence suggests that SIN could attenuate renal fibrosis through Nrf2-mediated inhibition of oxidative stress and TGF-β1 signaling [25]. Given the involvement of oxidative stress and TGF-β1 signaling in the pathogenesis of pulmonary fibrosis [26,27], the hypothesis emerges that SIN may exhibit anti-lung fibrosis functions. In this study, we utilized a well-established BLM-induced pulmonary fibrosis model to evaluate the therapeutic efficacy of SIN. Oral administration of SIN significantly mitigated pulmonary fibrosis in mice without detectable side effects. Importantly, SIN treatment resulted in a reduction in extracellular matrix deposition, diminished hydroxyproline contents, improved Ashcroft scores, and enhanced lung function parameters. These findings underscore the potential of SIN as a therapeutic agent for pulmonary fibrosis. Nevertheless, the precise mechanism by which SIN treats pulmonary fibrosis remains elusive.

There is rapidly growing evidence showing that the parallel relationship between fibroblast-to-myofibroblast differentiation and metabolic reprogramming [9,10,28]. Specifically, Aerobic glycolysis plays a pivotal role in driving fibroblast-to-myofibroblast differentiation, thereby contributing to the pathogenesis of pulmonary fibrosis. Through the upregulation of glycolytic enzymes and the generation of metabolic intermediates, aerobic glycolysis sustains the energetic demands and biosynthetic requirements of myofibroblasts, facilitating their phenotypic transition and promoting fibrotic tissue remodeling [11]. This metabolic reprogramming not only fuels the heightened proliferative and synthetic activities of myofibroblasts but also enhances their resistance to apoptosis, thereby perpetuating fibrosis progression [11]. Consequently, the inhibition of aerobic glycolysis, as demonstrated by 2-Deoxy--D-glucose (2-DG), significantly attenuates fibroblast activation and pulmonary fibrosis progression [11]. Our study contributes novel insights into the regulation of aerobic glycolysis by SIN in the context of pulmonary fibrosis. Utilizing the Seahorse Bioscience Extracellular Flux Analyzer, we observed that SIN reverses TGF-β1-induced aerobic glycolysis in fibroblasts. Mechanistically, SIN achieves this by specifically suppressing the expression of Pfkfb3, a key enzyme stimulating glycolysis. The significance of Pfkfb3 in SIN's anti-fibrotic effects was further confirmed by Pfkfb3 overexpression experiments, which reversed the protective effects of SIN on fibroblast-to-myofibroblast differentiation. Given the pivotal role of PFKFB3 in diseases such as pulmonary arterial hypertension, cardiac fibrosis, diabetes, nasopharyngeal carcinoma, and pulmonary injury, we hypothesize that SIN may exhibit therapeutic effects on the aforementioned conditions. However, the exact mechanisms underlying SIN's inhibition of Pfkfb3 during myofibroblast formation remain unknown, representing a focus for future research.

In conclusion, our study positions SIN as a promising anti-fibrotic agent for pulmonary fibrosis. The nuanced regulatory role of SIN in aerobic glycolysis, specifically through Pfkfb3 inhibition, adds a layer of mechanistic depth to its therapeutic profile. Further clinical investigations are warranted to validate the safety and efficacy of SIN in human subjects, thereby bridging the translational gap and addressing the unmet medical needs in IPF.

Availability of data

The datasets used during the current study are available from the figshare (10.6084/m9. figshare.25952464).

CRediT authorship contribution statement

Zuqiong Nie: Methodology, Data curation, Conceptualization. **Jing Wu:** Writing – original draft, Visualization, Methodology. **Jun Xie:** Writing – original draft, Project administration, Data curation. **Wanling Yin:** Writing – review & editing, Supervision, Funding acquisition.

Declaration of competing interest

The authors declare the following financial interests/personal relationships which may be considered as potential competing interests:Wanling Yin reports financial support was provided by The Central Hospital of Wuhan. If there are other authors, they declare that they have no known competing financial interests or personal relationships that could have appeared to influence the work reported in this paper.

Acknowledgment

This study was supported by Scientific Research Fund of Wuhan Municipal Health and Family Planning Commission (No. WX19B01).

Appendix A. Supplementary data

Supplementary data to this article can be found online at https://doi.org/10.1016/j.heliyon.2024.e33314.

References

[1] A.J. Podolanczuk, C.C. Thomson, M. Remy-Jardin, L. Richeldi, F.J. Martinez, M. Kolb, et al., Idiopathic pulmonary fibrosis: state of the art for 2023, Eur. Respir. J. 61 (2023).
[2] Y. Wang, L. Zhang, T. Huang, G.R. Wu, Q. Zhou, F.X. Wang, et al., The methyl-CpG-binding domain 2 facilitates pulmonary fibrosis by orchestrating fibroblast to myofibroblast differentiation, Eur. Respir. J. 60 (2022).
[3] Y. Hu, Q. Wang, J. Yu, Q. Zhou, Y. Deng, J. Liu, et al., Tartrate-resistant acid phosphatase 5 promotes pulmonary fibrosis by modulating beta-catenin signaling, Nat. Commun. 13 (2022) 114.
[4] X. Guo, O. Adeyanju, C. Sunil, V. Mandlem, A. Olajuyin, S. Huang, et al., DOCK2 contributes to pulmonary fibrosis by promoting lung fibroblast to myofibroblast transition, Am. J. Physiol. Cell Physiol. 323 (2022) C133–C144.
[5] Z. Zheng, F. Peng, Y. Zhou, Pulmonary fibrosis: a short- or long-term sequelae of severe COVID-19? Chin Med J Pulm Crit Care Med 1 (2023) 77–83.
[6] M.V. Plikus, X. Wang, S. Sinha, E. Forte, S.M. Thompson, E.L. Herzog, et al., Fibroblasts: origins, definitions, and functions in health and disease, Cell 184 (2021) 3852–3872.
[7] D. Li, Z. Zhong, C.N. Ko, T. Tian, C. Yang, From mundane to classic: sinomenine as a multi-therapeutic agent, Br. J. Pharmacol. (2023).

[8] W. Liu, X. Yu, L. Zhou, J. Li, M. Li, W. Li, et al., Sinomenine inhibits non-small cell lung cancer via downregulation of hexokinases II-mediated aerobic glycolysis, OncoTargets Ther. 13 (2020) 3209–3221.
[9] S. Mei, Q. Xu, Y. Hu, R. Tang, J. Feng, Y. Zhou, et al., Integrin beta3-PKM2 pathway-mediated aerobic glycolysis contributes to mechanical ventilation-induced pulmonary fibrosis, Theranostics 12 (2022) 6057–6068.
[10] W. Wang, Y. Zhang, W. Huang, Y. Yuan, Q. Hong, Z. Xie, et al., Alamandine/MrgD axis prevents TGF-beta1-mediated fibroblast activation via regulation of aerobic glycolysis and mitophagy, J. Transl. Med. 21 (2023) 24.
[11] N. Xie, Z. Tan, S. Banerjee, H. Cui, J. Ge, R.M. Liu, et al., Glycolytic reprogramming in myofibroblast differentiation and lung fibrosis, Am. J. Respir. Crit. Care Med. 192 (2015) 1462–1474.
[12] T. Pan, Q. Zhou, K. Miao, L. Zhang, G. Wu, J. Yu, et al., Suppressing Sart1 to modulate macrophage polarization by siRNA-loaded liposomes: a promising therapeutic strategy for pulmonary fibrosis, Theranostics 11 (2021) 1192–1206.
[13] F. Ahangari, C. Becker, D.G. Foster, M. Chioccioli, M. Nelson, K. Beke, et al., Saracatinib, a selective src kinase inhibitor, blocks fibrotic responses in preclinical models of pulmonary fibrosis, Am. J. Respir. Crit. Care Med. 206 (2022) 1463–1479.
[14] Q. Wang, J. Liu, Y. Hu, T. Pan, Y. Xu, J. Yu, et al., Local administration of liposomal-based Srpx2 gene therapy reverses pulmonary fibrosis by blockading fibroblast-to-myofibroblast transition, Theranostics 11 (2021) 7110–7125.
[15] R. Guan, L. Yuan, J. Li, J. Wang, Z. Li, Z. Cai, et al., Bone morphogenetic protein 4 inhibits pulmonary fibrosis by modulating cellular senescence and mitophagy in lung fibroblasts, Eur. Respir. J. 60 (2022).
[16] T. Huang, J. Song, J. Gao, J. Cheng, H. Xie, L. Zhang, et al., Adipocyte-derived kynurenine promotes obesity and insulin resistance by activating the AhR/STAT3/IL-6 signaling, Nat. Commun. 13 (2022) 3489.
[17] P. Solopov, R. Biancatelli, M. Marinova, C. Dimitropoulou, J.D. Catravas, The HSP90 inhibitor, AUY-922, ameliorates the development of nitrogen mustard-induced pulmonary fibrosis and lung dysfunction in mice, Int. J. Mol. Sci. 21 (2020).
[18] D. Wu, X. Fu, Y. Zhang, Q. Li, L. Ye, S. Han, et al., The protective effects of C16 peptide and angiopoietin-1 compound in lipopolysaccharide-induced acute respiratory distress syndrome, Exp Biol Med (Maywood) 245 (2020) 1683–1696.
[19] H. Zhong, R. Tang, J.H. Feng, Y.W. Peng, Q.Y. Xu, Y. Zhou, et al., Metformin mitigates sepsis-associated pulmonary fibrosis by promoting AMPK activation and inhibiting Hif-1alpha-induced aerobic glycolysis, Shock 61 (2024) 283–293.
[20] Q. Wang, J. Yu, Y. Hu, X. Chen, L. Zhang, T. Pan, et al., Indirubin alleviates bleomycin-induced pulmonary fibrosis in mice by suppressing fibroblast to myofibroblast differentiation, Biomed. Pharmacother. 131 (2020) 110715.
[21] G.A. Margaritopoulos, E. Vasarmidi, K.M. Antoniou, Pirfenidone in the treatment of idiopathic pulmonary fibrosis: an evidence-based review of its place in therapy, Core Evid. 11 (2016) 11–22.
[22] J. Li, J. Cao, Q. Chen, D. Liu, R. Li, Investigating the therapeutic potential of sinomenine in rheumatoid arthritis: anti-inflammatory, antioxidant, and immunomodulatory mechanisms, Naunyn-Schmiedeberg's Arch. Pharmacol. 397 (2024) 3945–3958.
[23] J. Zhu, H. Zhu, J. Gao, The anti-tumor potential of sinomenine: a narrative review, Transl. Cancer Res. 12 (2023) 2393–2404.
[24] H. Fan, Y. Yang, Q. Bai, D. Wang, X. Shi, L. Zhang, et al., Neuroprotective effects of sinomenine on experimental autoimmune encephalomyelitis via anti-inflammatory and nrf2-dependent anti-oxidative stress activity, NeuroMolecular Med. 25 (2023) 545–562.
[25] T. Qin, S. Yin, J. Yang, Q. Zhang, Y. Liu, F. Huang, et al., Sinomenine attenuates renal fibrosis through Nrf2-mediated inhibition of oxidative stress and TGFbeta signaling, Toxicol. Appl. Pharmacol. 304 (2016) 1–8.
[26] R. Zhou, C. Jin, L. Jiao, S. Zhang, M. Tian, J. Liu, et al., Geranylgeranylacetone, an inducer of heat shock protein 70, attenuates pulmonary fibrosis via inhibiting NF-kappaB/NOX4/ROS signalling pathway in vitro and in vivo, Chem. Biol. Interact. 382 (2023) 110603.
[27] L.Z. Rao, Y. Wang, L. Zhang, G. Wu, L. Zhang, F.X. Wang, et al., IL-24 deficiency protects mice against bleomycin-induced pulmonary fibrosis by repressing IL-4-induced M2 program in macrophages, Cell Death Differ. 28 (2021) 1270–1283.
[28] J. Zhang, W. Chen, J. Du, L. Chu, Z. Zhou, W. Zhong, et al., RNF130 protects against pulmonary fibrosis through suppressing aerobic glycolysis by mediating c-myc ubiquitination, Int. Immunopharm. 117 (2023) 109985.